Journal of Electroanalytical Chemistry 957 (2024) 118105

Contents lists available at ScienceDirect

Journal of Electroanalytical Chemistry

journal homepage: www.elsevier.com/locate/jelechem

The sloped limiting current region during ion transfer at arrays of nanointerfaces between immiscible electrolyte solutions

Mickaël Rimboud [a,b], Benjamin J.J. Austen [a], Jörg Strutwolf [c], Yang Liu [a,d], Damien W. M. Arrigan [a,*]

[a] School of Molecular and Life Sciences, Curtin University, GPO Box U1987, Perth, Western Australia 6845, Australia
[b] Laboratoire des Matériaux et Molécules en Milieu Agressif (L3MA) UR4-1, Université des Antilles, Campus de Schoelcher, 97233 Schoelcher, Martinique, France
[c] Institute for Print and Media Technology, Department of Mechanical Engineering, Chemnitz University of Technology, D-09126 Chemnitz, Germany
[d] College of Science and Engineering, James Cook University, Townsville, Queensland, 4811, Australia

ARTICLE INFO

Keywords:
Interface
ITIES
Nanopore
Array
Voltammetry
Ternary electrodiffusion

ABSTRACT

The formation of arrays of nano-interfaces between immiscible electrolyte solutions using nanoporous membranes opens up new opportunities in electrochemical analysis. However, an unusual feature in the voltammetry, in the form of a consistently sloped current in the limiting current region, has been observed. This sloped limiting current was observed using different alkylammonium cation transfers at the nanoITIES arrays, showing the generality of the feature. Experiments with variable concentrations of organic or aqueous phase electrolytes revealed that the sloped limiting current was impacted by the concentration of the aqueous phase electrolyte. A plausible explanation for the effect is discussed based on ternary electrodiffusion which occurs due to facilitated ion transfer of the aqueous phase background electrolyte cation. As a result, the use of nanoITIES arrays as the basis for chemical sensors and detection needs to be carefully considered.

1. Introduction

Electrochemistry at the interface between two immiscible electrolyte solutions (ITIES) brings scope to electroanalysis and sensor development by the opportunity to apply a broad range of experimental techniques to study and detect ion transfer processes at liquid–liquid interfaces [1–4]. A range of ions or ionisable substances can be detected by simple ion transfer or facilitated ion transfer (FIT) processes at interfaces formed between aqueous and organic electrolyte solutions. Thus, detection of a range of organic compounds that are ionised or ionisable have been studied by these approaches by various groups, as summarised in recent reviews [2,3]. Inorganic substances, especially metal cations, have been the subject of a variety of FIT processes for detection purposes [5,6]. In parallel with the investigation of the detection capabilities of electrochemistry at the ITIES for analytes of biological interest, interface miniaturisation [1] to the microscale and the nanoscale[7] has developed rapidly, initially by location of the ITIES at the mouth of a micropipette [8,9] or nanopipette [10], and subsequently by location of the ITIES at the pores of micro- or nano-sized porous membranes [1] prepared by methods such as laser photoablation [6], photolithography/reactive ion etching [11], electron-beam lithography/reactive ion etching (EBL/RIE) [12], focused ion beam milling [13] and nuclear track etching [14]. In particular, we have investigated EBL/RIE-fabricated nanoporous silicon nitride membranes for patterning of the ITIES into an array of nanoscale ITIES [12,15–17]. Such nanoITIES arrays brought improved detection sensitivities when targeted to model ions, such as alkylammonium cations [15] as well as the drug propranolol [18].

In a previous paper [16], we described the transfer of tetraethylammonium cation (TEA^+) using different nanopore array-supported water|1,6-dichlorohexane (DCH) interfaces. The nanopore arrays displayed five different pore sizes, from 17 to 75 nm radius (r_a), with 400 pores and a ratio between the pore–pore distance (r_c) and the pore radius of 20. It was shown that the nanoITIES array so-formed behaved like an inlaid nanoelectrode array, i.e. the pores were filled with the organic phase, and that the analytical sensitivity improved as the pore size decreased. However, the ion transfer voltammograms obtained with these nanopore array-based ITIES displayed a slight current rise instead of a true current plateau as a common feature. Particularly, the voltammograms observed with the two smallest pore radii, 20 and 17 nm, showed unusual behaviour: there was no apparent change in current

* Corresponding author.
E-mail address: d.arrigan@curtin.edu.au (D.W.M. Arrigan).

https://doi.org/10.1016/j.jelechem.2024.118105
Received 11 December 2023; Received in revised form 30 January 2024; Accepted 5 February 2024
Available online 7 February 2024

slope between the ion transfer wave and the background (electrolyte transfer) current. Instead, the current exhibited a continuous rise from the ion transfer current, and no plateau or inflexion was distinguished. We refer to this current region as the "sloped limiting current region" (SLCR). On the reverse scan of cyclic voltammograms, a broad peak of negative current was observed, which could be very distorted and stretched on the potential axis. In some experiments, crossings between forward and backward scans and a nucleation loop appeared [16].

Here, we report the results of investigations aimed to understand the origin of this sloped limiting current behaviour, especially the identification of the experimental parameters that contributed to the sloped limiting current, and whether the observation depended on the pore sizes used to define the nanoITIES array. Firstly, the voltammetry of different tetraalkylammonium cation transfers from aqueous phase to a 1,6-dichlorohexane phase was examined, using the nanopore designs with r_a of 75 and 25 nm (designs 1 and 3, respectively), paying attention to the sloped limiting current region, in order to determine if there was a dependence of this slope on the pore size. Secondly, the role of electrolyte concentration in either phase was examined to see whether this influences the ion transfer current at arrays of larger and smaller pores (r_a = 75, 25 or 17 nm, designs 1, 3, 5, respectively).

2. Experimental

2.1. Reagents and materials

All reagents used were purchased from Sigma-Aldrich Australia and used without further purification unless indicated otherwise here. Deionised water was obtained from a Milli-Q water purification system (Millipore Pty Ltd, North Ryde, NSW, Australia). The water produced by this unit had a resistivity of 18 MΩ.cm. The solvent employed for the organic phase was 1,6-dichlorohexane (DCH) [19,20]. It was rinsed three times with deionised water prior to use. Both the water and DCH were mutually saturated before further use. The supporting electrolytes were LiCl in the aqueous phase and bis(triphenylphosphoranylidene) ammonium tetrakis(4-chlorophenyl)borate (BTTPATPBCl) in DCH, both at a concentration of 10 mM unless specified otherwise. The latter salt was prepared by metathesis from bis(triphenylphosphoranylidene) ammonium chloride (BTTPACl) and potassium tetrakis(4-chlorophenyl) borate (KTPBCl), following the published procedure [6]. The tetraalkylammonium (TAA^+) salts employed were chlorides (tetramethyl-, tetraethyl- and tetrapropylammonium (TMA^+, TEA^+, TPA^+)) or bromide (tetrabutylammonium (TBA^+)).

The preparation of the silicon nitride nanopore array membranes (of thickness 100 nm) used to form the nano-interfaces was described previously [12], and used combinations of photolithography and EBL/RIE, etching and deposition. As summarised in Table 1, the arrays all consisted of 400 nanopores, with r_c/r_a = 20, and r_a values of 75, 25 or 17 nm, referred to here as designs 1, 3 and 5, respectively, in keeping with the previous report [16].

2.2. Experimental procedure

Voltammetric experiments at nanopore-supported liquid–liquid interface arrays were performed using an Autolab PGSTAT302N (Metrohm, The Netherlands) together with Nova 1.7 software. A two-electrode electrochemical cell was used, with both electrodes serving as reference and counter electrode in either phase. This was possible because of the low currents measured. The organic phase (200 μL) was contained in a glass tube (2.5 mm inner and 4 mm outer diameter) with the silicon nitride membrane on a chip (5 mm x 5 mm) sealed to one end with silicone sealant. This was then immersed in the aqueous phase (3 mL) contained in a 10 mL beaker. In experiments with reference electrodes (Cell 1), an aqueous solution of LiCl (0.01 M) saturated in BTPPACl was placed on top of the organic phase with a silver/silver chloride wire. The electrochemical cells used are summarised in Scheme 1.

In most experiments, however, a silver wire was placed directly into the organic phase (Cell 2), acting as a pseudo-reference electrode, to simplify the experimental set-up. The voltammograms recorded with Cell 2 were then transposed to correspond to those obtained with Cell 1, by standardisation with the half-wave transfer potential of the analysed ion. All potential values reported here are with respect to the silver/silver chloride reference electrode.

Once the cell was set up, a background voltammogram was run over a wide potential range in order to establish the available potential window; this shifted slightly with each experiment when a pseudo-reference electrode was used. A sequence of three successive "blank" (background) voltammograms was subsequently recorded in a potential range large enough to encompass the transfer of the analyte ion when it was added to the aqueous phase. Aliquots of a 1 mM TAAX solution in 0.01 M LiCl in DCH-saturated water were then added to the aqueous phase with a micropipet in order to produce the desired concentration of TAA^+ in the aqueous phase. For all experiments, cells were placed in a Faraday cage and voltammetric experiments were performed at a scan rate of 5 mV s^{-1}.

Table 1
Geometric characteristics of the silicon nitride nanopore arrays employed to prepare the arrays of nanoITIES [16].

Parameter	*Design 1*	*Design 3*	*Design 5*
Radius of pore, r_a/nm	75	25	17
Distance between pores, r_c/nm	1500	500	300
Number of pores, N_p	400	400	400

3. Results and discussion

3.1. Sloped limiting current

The voltammograms obtained for the transfer of the four different tetraalkylammonium cations with array design 1 (r_a = 75 nm) are presented in Fig. 1A. Table 1 summarises the array designs employed. Fig. 1A also shows equivalent blank voltammograms (i.e. no analyte ion transfer). The corresponding forward scans after background subtraction are presented in Fig. 1B. As expected, the ions transferred in the order of their affinity for the organic phase: TBA^+, the more hydrophobic species, transferred at the lowest potential ($E_{1/2}$ = 0.41 V, curve 4) and TMA^+, the more hydrophilic species, transferred at the highest potential ($E_{1/2}$ = 0.82 V, curve 1). As the individual interfaces were equivalent to inlaid disc electrodes, the theoretical limiting current observed for the transfer of an ion j can be ideally calculated using the formula [21,22]:

$$I_{lim} = 4N_p|z_j|FD_jC_jr_a \quad (1)$$

in which I_{lim} is the limiting current, N_p the number of pores used to form the nanoITIES array, F is the Faraday constant, r_a is the interfacial radius, and z_j, D_j and C_j are, respectively, the charge, the diffusion coefficient and the bulk concentration of ion j. The experimental currents are ca. 50 % lower than the calculated values because of diffusion zone overlap in these nanopore array designs, as discussed previously [16,23]. However, as the TAA^+ ions are present in aqueous phase at the same concentration, the differences observed between their respective limiting currents are due to their different diffusion coefficients. Values of these diffusion coefficients from the literature are compiled in Table 2. As expected, the largest ion, TBA^+, diffuses more slowly than the others ($D^+_{w,TBA} = 5.2 \times 10^{-6}$ cm^2 s^{-1}) [24], and so the corresponding limiting current is lower; the opposite is observed for TMA^+, which diffuses faster than the other three species ($D^+_{w,TMA} = 9.5 \times 10^{-6}$ cm^2 s^{-1}) [25] and so the corresponding limiting current is higher. Similar observations were made when using nanopore design 3 (r_a = 25 nm,

Cell 1:

Ag|AgCl|LiCl (0.01 M), BTPPACl sat. W | BTTPATPBCl (x M) DCH || LiCl (x M) W|AgCl|Ag

Cell 2:

Ag|BTTPATPBCl (x M) DCH || LiCl (x M) W|AgCl|Ag

Scheme 1. Electrochemical cells employed in these experiments. W, DCH refer to aqueous and organic phases, respectively; x indicates the concentration of electrolyte in aqueous or organic phase. The studied interface is indicated by the double vertical bars.

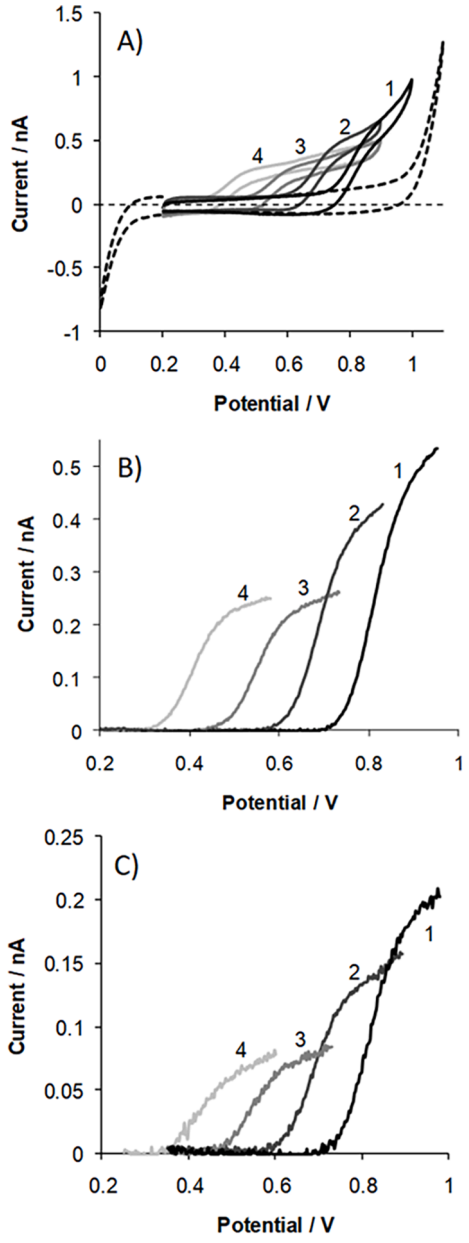

Fig. 1. Cyclic voltammetry of 100 μM of TMACl (1), TEACl (2), TPACl (3) and TBABr (4) at W-DCH interface obtained with array design 1 (r_a = 75 nm, A: experimental cyclic voltammograms, B: forward scan after background-subtraction) and design 3 (r_a = 25 nm, C: forward scan after background-subtraction).

Table 2
Diffusion coefficients of the four TAA^+ ions ($\times 10^6$ cm^2 s^{-1}).

TBA^+	TPA^+	TEA^+	TMA^+
5.2 [24]	7.5 [26]	7.9 [27]	9.5 [25]

Table 1), for which the background-subtracted forward scan voltammograms are shown in Fig. 1C. As predicted from theory and from our previous work [16], a ratio of ca. 3 is observed when comparing the limiting currents obtained for any given TAA^+ with the two different nanopore sizes. This ratio corresponds to the ratio of the corresponding pore radii, 75 nm for design 1 and 25 nm for design 3 (Table 1).

However, it is noticeable that no true current plateaus are observed following the transfer wave in both nanoITIES array (Fig. 1). It can be readily seen, in all cases, that the current continues to increase steadily. We refer to this characteristic as the sloped limiting current. To get a better appreciation of this phenomenon, the slopes of these limiting current regions for each cation and array design (1 and 3) were measured on the background-subtracted forward scans (as described in Fig. 2A); the slope values obtained are summarised in Fig. 2B.

The values of these current slopes increased in the following ion sequence: $TBA^+ < TPA^+ < TEA^+ < TMA^+$, for both nanopore design 1 (dark grey bars) and 3 (light grey bars). The values of the slopes were, respectively, 0.30, 0.37, 0.80 and 0.91 nA V^{-1} for TBA^+, TPA^+, TEA^+ and TMA^+ with design 1, and 0.18, 0.15, 0.27 and 0.34 nA V^{-1} with design 3. As these current slopes were measured on background-subtracted curves, it suggests that they are not related to the proximity of the ion transfer process to the transfers of supporting electrolyte ions (which sets the upper limit of the available potential window). The current slopes increased in a similar ascending order as the diffusion coefficients of the four TAA^+ species. On comparison of the slopes for each TAA^+ species at both pore designs, the ratios of these slopes close to 3, which corresponds to the ratio of the pore radii for the two designs (Table 1). When considering the two largest ions, TBA^+ and TPA^+, no experimental difference was observed for the current slopes at both designs 1 and 3 (Fig. 2B). Nevertheless, the data present a trend in the magnitude of the slope with the ions studied. These observations seem to link the sloping current values to both the ion diffusion coefficients and to the size of the nano-interfaces, although it must be pointed out that for these nanoITIES array designs, diffusion to the entire arrays occurs due to diffusion zone overlap. Separate studies of ion-transfer voltammetry of protonated propranolol [18] at similar nanoITIES arrays to those used here (prepared with nanopore array membranes with r_a values of 50 nm or 17 nm, $r_c/r_a = 20$, and 400 nanopores in hexagonal array) and of TEA^+ transfer at nanoITIES arrays employing FIB-milled pores [28] in various ratios of r_c/r_a also displayed the sloped limiting current region. In these studies, the sloped limiting current was found to be concentration dependent in the range 20–100 μM [18,28].

Previously, Dale and Unwin [29] observed a similar phenomenon at a single micrometre-sized ITIES: a slight increase of the current after the ion transfer wave instead of a steady state plateau. They attributed this

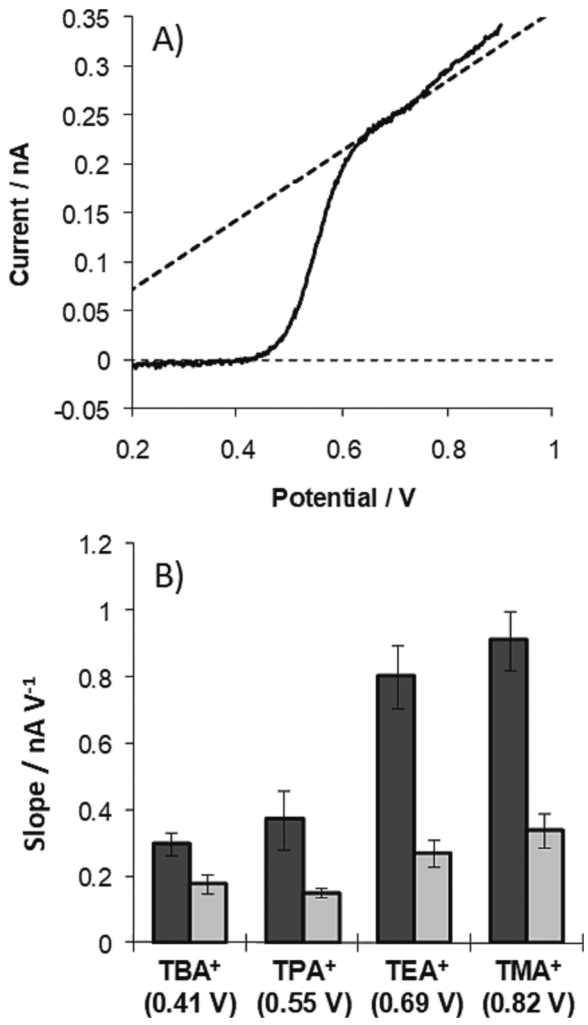

Fig. 2. Comparison of the slopes of the current rising. A: determination of the slope. B: comparison of the slopes for the four TAA^+ ions using nanopore design 1 (dark grey) and 3 (light grey).

behaviour to a progressive expansion/contraction of the interface as the transfer progressed. As the interface becomes larger, the recorded currents increase and so a steady increase of the limiting current is observed. In theory, if the interface expanded up to the size of a hemisphere, the limiting current would be calculated by substituting 2π for the factor 4 in equation (1), which would become:

$$I_{lim} = 2\pi N_p |z_j| F D_j C_j r_a \quad (2)$$

The limiting current would then increase upto a limit of $2\pi/4$ times (i.e. an increase of current by upto 1.57 times that for an inlaid disc) during the expansion of the interface. In reality, the current could be increased within the range between that for an inlaid disc interface and that for a hemispherical interface, depending on the extent of the interface expansion. It seems then logical to postulate that the current rise will be higher for a more rapidly-diffusing ion. Moreover, a larger interface will show a higher current but a lower interfacial tension and be more easily deformable than a small one. These observations might explain why the current slopes are smaller with nanopore design 3 (r_a = 25 nm) than with design 1 (r_a = 75 nm) and why a ratio close to the nanopore size ratio is observed when comparing them.

These results demonstrated a coherent behaviour between array designs 1 and 3 as the pore size decreases. They also show that the sloped limiting current region is largest for the smallest ion at the larger interfaces.

3.2. Effect of the presence of supporting electrolytes

Due to the small size of the liquid–liquid interface, there might be an increased difficulty for the interface to rearrange and stabilise itself when ion transfer occurs so that the high flux of the transferring ions might destabilise the electrical double layer-like [30] structure at the interface. Accordingly, the relative size of the different ions in solution compared to the interface would be critical. By altering the concentration of the other ions in solution, i.e. the supporting electrolytes, the rearrangement of the interface subjected to ion transfer could be expected to change and so a change of the magnitude of the current slope could be anticipated. In the case of nanopore design 5 (r_a = 17 nm, Table 1), we would expect to observe an inflexion between the ion-transfer wave and the background current rise. As the supporting electrolyte ions in the organic phase, $BTPPA^+$ and $TPBCl^-$, are larger than those in water, Li^+ and Cl^-, (see Table 3 for data on ion sizes) we anticipated that their presence at lower concentrations would have a greater impact on the current rise. Therefore, the transfer of 10^{-4} M of TEA^+ across the W|DCH interface was studied with three nanopore array designs (designs 1, 3 and 5, Table 1) and with three concentrations of supporting electrolyte in either the aqueous or the DCH phase.

3.2.1. BTPPATPBCl in DCH

The voltammograms obtained for concentrations of BTPPATPBCl in DCH of 10^{-4}, 10^{-3} and 10^{-2} M with each of the array designs are shown in Fig. 3. There are marked differences between the voltammograms obtained with array designs 1 and 3 on the one hand (Fig. 3, A to F) and those obtained with design 5 on the other (Fig. 3, G to I), as found in our previous work [16]. When design 5 is used (r_a = 17 nm), a continuous increase of the background current, convoluted with the TEA^+ transfer wave, is observed rather than a current plateau following the transfer wave. On the reverse scan, a large and distorted negative current peak is observed before the current returns to its initial "blank" value. No inflexion is observed on the current rise as the concentration of BTPPATPBCl in the organic phase decreases from 10^{-2} (Fig. 3I) to 10^{-3} and 10^{-4} M (Fig. 3H and 3G, respectively).

Different concentrations of supporting electrolyte in DCH cause a change in the background current for each of the array designs. This is observed (Fig. 3) both when TEA^+ is transferring (solid line) and in the corresponding blank voltammograms (dotted line) with no TEACl present in the aqueous phase. When array design 1 is used (r_a = 75 nm), the background current measured at 0.45 V (before the TEA^+ transfer wave) for a blank CV increased from 0.12 nA in 10^{-2} M supporting electrolyte (Fig. 3C) to 0.15 and 0.33 nA in 10^{-3} M and 10^{-4} M electrolyte, respectively (Fig. 3B and 3A). So the background current more than doubled as the concentration of BTPPATPBCl in DCH decreased 100-fold. The same trend is visible with the other two array designs, the background current increased from 0.07 nA to 0.27 nA and from 0.08 nA to 0.34 nA with designs 3 (Fig. 3F and 3D) and 5 (Fig. 3I and 3G), respectively, as the concentration of electrolyte decreased 100-fold.

Following background subtraction (curves not shown), the limiting currents with arrays design 1 and 3 remained essentially independent of

Table 3
Ionic radii of the ions employed in this work.

Ion	Radius/Å	Reference
Li^+	0.60	[31]
Cl^-	1.81	[31]
Br^-	1.95	[31]
TMA^+	3.47	[32]
TEA^+	4.00	[32]
TPA^+	4.52	[32]
TBA^+	4.94	[32]
$BTTPA^+$	6.60 9.90	[33]
$TPBCl^-$	5.0	[34], estimated value

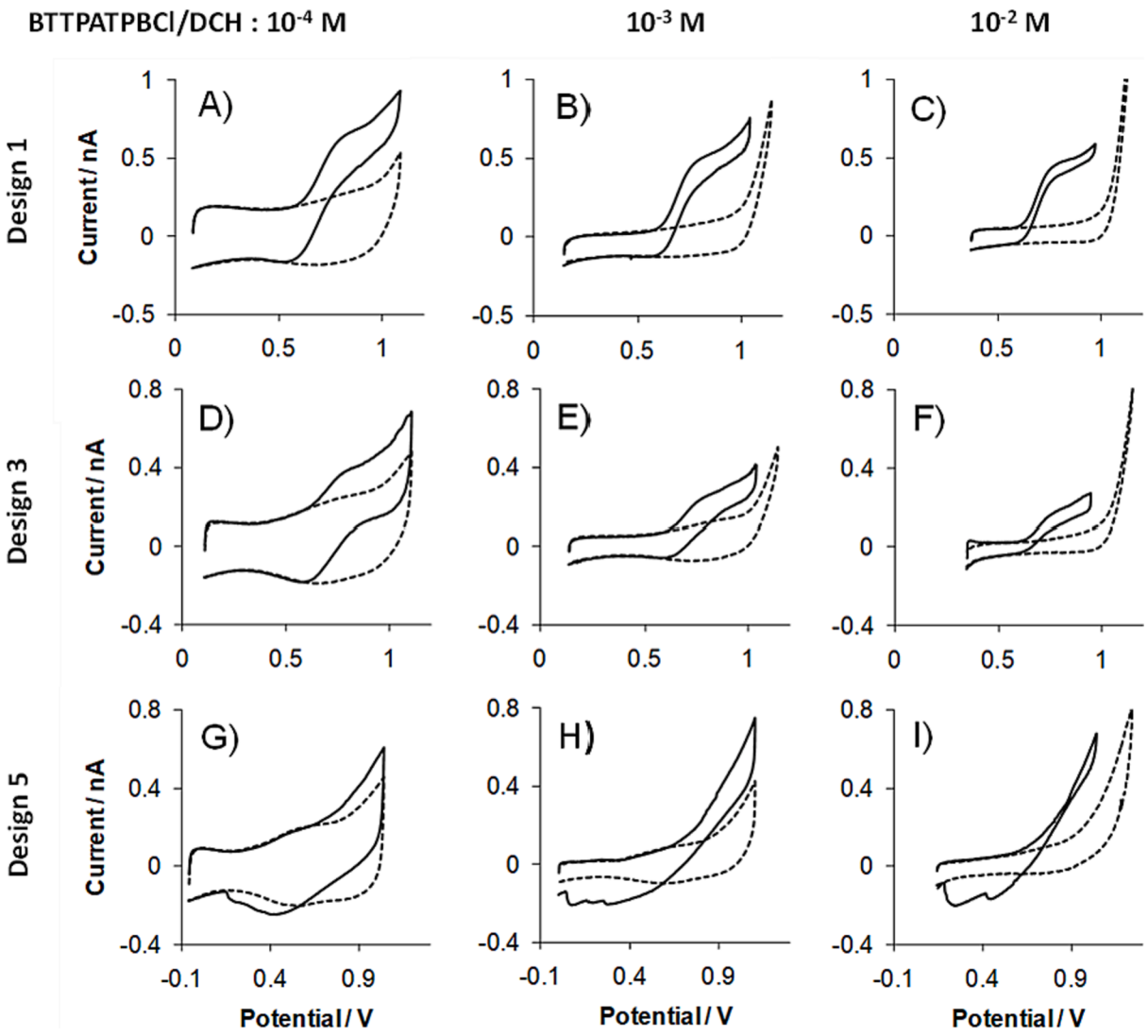

Fig. 3. Transfer of 100 μM of TEACl at W-DCH interface using nanopore design 1 (A, B, C), 3 (D, E, F) or 5 (G, H, I) and 10^{-4} (A, D, G), 10^{-3} (B, E, H) or 10^{-2} M (C, F, I) of BTPPATPBCl in DCH (solid lines). Dotted lines: Voltammograms in the absence of TEACl.

organic phase electrolyte concentration (0.42 and 0.15 nA for array designs 1 and 3, respectively) for the three concentrations of BTPPATPBCl studied. This observation is in accordance with previous work [35]: in order for the supporting electrolyte concentration to introduce a migration current for the analyte, it must be in the same phase as the analyte. In the experiment here, the variable electrolyte concentrations are in the adjoining phase to that of the analyte. Another effect expected with lower concentration of organic phase supporting electrolyte was an increased organic phase resistance that should manifest itself as a distortion of the voltammogramms along the potential axis. This phenomenon is obvious in the data here: the curves obtained with 10^{-2} M or 10^{-3} M organic supporting electrolyte and array design 1 (r_a = 75 nm) or 3 (r_a = 25 nm) are mostly identical (Fig. 3C, 3B for design 1; Fig. 3F, 3E, for design 3), but the voltammograms obtained with 10^{-4} M of BTPPATPBCl (Fig. 3A and 3D) were distorted. The same conclusions can be made concerning array design 5 (r_a = 17 nm) as the voltammograms with 10^{-2} and 10^{-3} M organic supporting electrolyte are similar after background-subtraction, but the voltammogram obtained in 10^{-4} M was distorted along the potential axis, which is attributed to the increased resistance of the organic phase.

The slope of the limiting current after the TEA^+ transfer wave showed no apparent trend with the concentration of organic phase supporting electrolyte. Furthermore, across all organic electrolyte concentrations, the mean slope was 0.26 nA V^{-1} (range 0.19–0.32 nA V^{-1}) with nanopore design 1 (r_a = 75 nm) and 0.26 nA V^{-1} (range 0.22–0.29 nA V^{-1}) with nanopore design 3 (r_a = 25 nm) (mean values calculated from the voltammograms obtained at the three different BTTPATPBCl concentrations). However, for the smallest nanopore radius (Design 5, (r_a = 17 nm), there was no visible change in the current rise as the organic electrolyte concentration was changed. These observations indicate that altering the electrolyte concentration in the organic phase does not impact the slope of the limiting current rise, but does introduce other effects (and these other effects may be capacitive or resistive).

3.2.2. *LiCl in water*

A series of experiments in which the aqueous phase electrolyte concentration was varied were carried out. The voltammograms are shown in Fig. 4. The results obtained with nanopore array design 5 (r_a = 17 nm) (Fig. 4G to 4I) differ from those obtained with array designs 1 and 3, as also described above. The different concentrations of aqueous supporting electrolyte (10^{-2} M, 10^{-3} M, 10^{-4} M LiCl) did not change the appearance of the voltammograms recorded with array design 5.

Contrary to the results obtained with the variation of BTPPATPBCl concentration in the organic phase, no significant change of the capacitive current was observed when the aqueous concentration of LiCl was

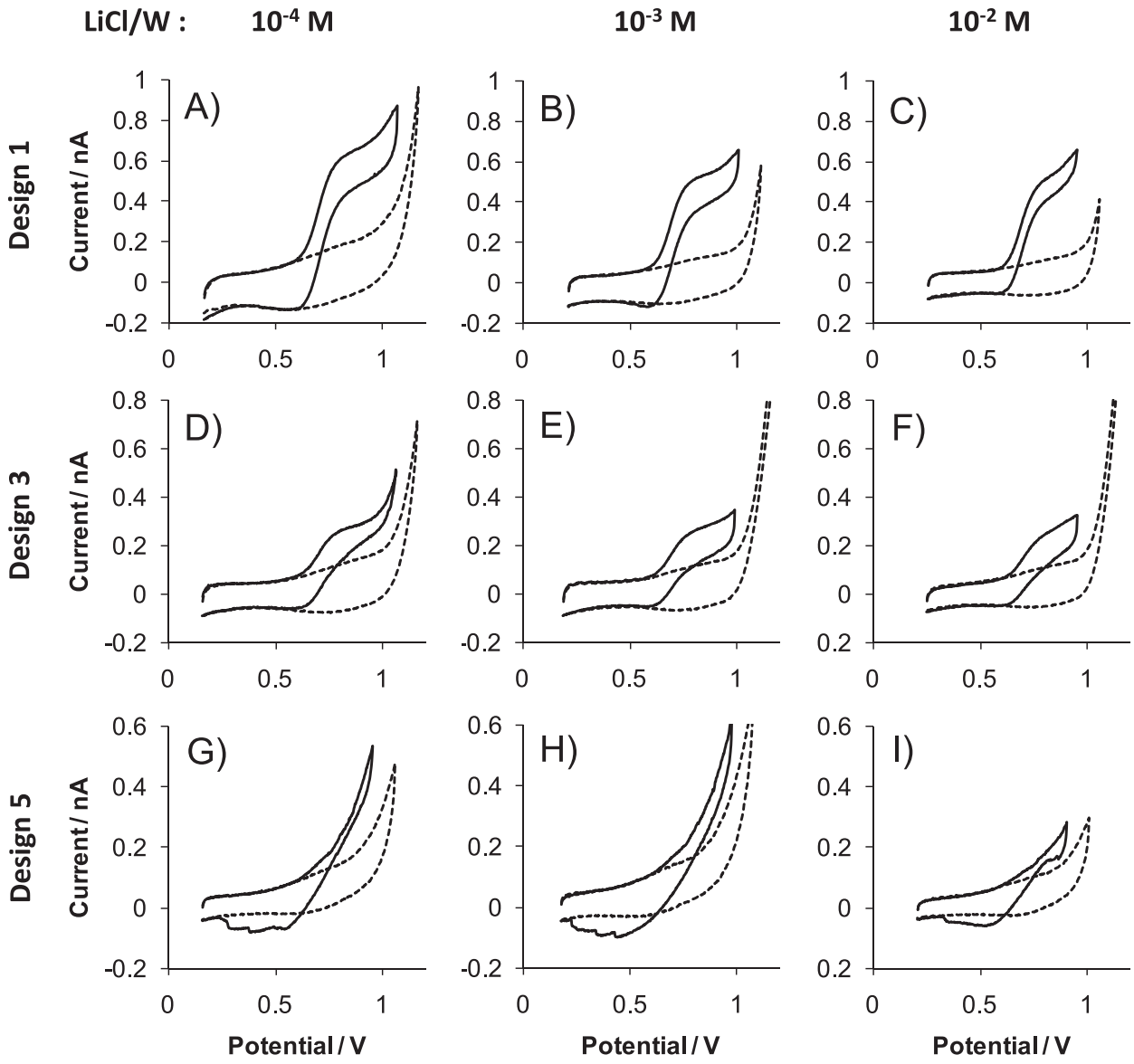

Fig. 4. Transfer of 100 μM of TEACl at W-DCH interface using nanopore design 1 (A, B, C), 3 (D, E, F) or 5 (G, H, I) and 10^{-4} (A, D, G), 10^{-3} (B, E, H) or 10^{-2} M (C, F, I) of LiCl in water (solid lines). Dotted lines: Voltammograms in the absence of TEACl.

decreased. A capacitive current of 0.11, 0.10 and 0.08 nA was measured at 0.45 V for array designs 1, 3 and 5, respectively.

The limiting current measured after background subtraction remained constant as the concentration of LiCl decreased for most of the experiments, 0.41 and 0.15 nA, respectively, for array designs 1 and 3. These values are the same as those measured with varying BTPPATPBCl concentration in the organic phase. A higher limiting current is observed only with array design 1 and the lower concentration of LiCl studied (10^{-4} M), 0.44 nA. This higher current is attributed to the contribution of migration of TEA^+ at this low concentration of electrolyte [35].

In contrast to the limiting current, however, the sloped limiting current region above the ion transfer wave exhibited a clear difference across the three concentrations of LiCl studied for both array designs 1 and 3. The forward scans obtained after background subtraction with array design 3 are presented in Fig. 5. With design 1, the slope is 0.16 nA V^{-1} when 10^{-4} M LiCl was used, but it increased to 0.24 nA V^{-1} with 10^{-3} M and 0.56 nA V^{-1} with 10^{-2} M. The same trend is observed with array design 3, the slopes being 0.02, 0.15 and 0.34 nA V^{-1} with, respectively, 10^{-4}, 10^{-3} and 10^{-2} M of LiCl in aqueous phase. The same trend as shown in Fig. 2 is also seen here for the slope value relative to the nanopore radius. These results suggest that the sloped limiting current region is associated with the aqueous electrolyte phase, although no such trend was seen with array design 5. With this design, the curves show no changes with the concentration of LiCl. No inflexion allowing the separation of the ion transfer from the background current was demonstrated, even with the lowest concentration of LiCl in water. Nevertheless, at the larger nanopore sizes, a clear dependence of the slope of the sloped limiting current region is seen on the aqueous phase electrolyte concentration.

These experiments demonstrate that our suggestion, that the size of the ions would impact the observed sloped limiting current, with a greater effect being expected for changes in organic electrolyte ion concentrations, was not plausible. No difference was evident from the voltammograms recorded with array design 5 (r_a = 17 nm) as the concentration of the supporting electrolyte, both BTPPATPBCl in the organic phase and LiCl in the aqueous phase, decreased. Contrary to expectations, the concentration of LiCl in water seems to have the greater impact on the current rise, as seen with array designs 1 and 3. This influence may be more related to the presence of the ions in the same phase as the analyte (in water) and their effect on the transport

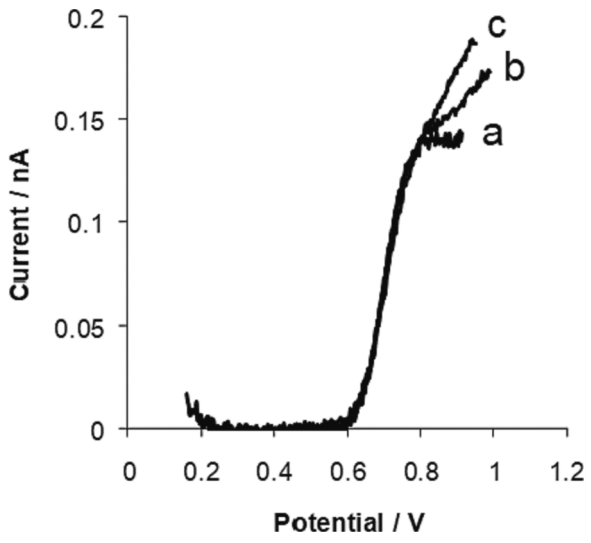

Fig. 5. Forward scan of the voltammograms of transfer of TEA^+ at W-DCH interface after background subtraction, using nanopore design 3 (25 nm radius) and 10^{-4} (a), 10^{-3} (b), or 10^{-2} M (c) of LiCl in water.

phenomenon rather than their relative size, that is, migrational effects occur in the aqueous phase.

3.3. General discussion

The experimental results presented above show that the sloped limiting current at nanoITIES arrays occurs following ion transfer from aqueous to organic phases. This occurrence is seen with ions that transfer at different applied potentials, resulting in the presence of the sloped limiting current at different potentials that are dependent on the transfer of each specific ion. One possibility for the cause of the sloped limiting current is the growth of the ITIES from an assumed inlaid planar nanodisc to a hemispherical nanoITIES during the course of the voltammetry, or anywhere in between: such a change would lead to an enhancement of the current by upto 1.57-times (see Eqs. (1) and (2)), depending on the extent of the interface expansion, although this increase would be offset by the overlap of diffusion zones at each nanoITIES, because at $r_c/r_a = 20$ the diffusion zones around each nanoITIES are not independent [23,28,36], and a resultant lower elevated current would ensue. In fact, the magnitude of the current increase from the start of the expected steady-state region (top of the wave) to the end of the steady-state region in the recorded voltammograms is ca. 20 %, not 57 %.

Background electrolyte effects were investigated, because amongst the possibilities considered were the disturbance of the electrical double layer at each nanoITIES due to deformation and reformation of the electrical double layer-like structures at the interfaces caused by the high flux of transferring ions. This deformation/reformation might lead to a potential-dependent capacitive current that is superimposed on the ion-transfer limiting current. Such a capacitive current is expected to depend on the concentration of the electrolyte ions in each phase. However, the sloped limiting currents were not dependent on the concentration of organic phase electrolyte but were dependent on the aqueous phase electrolyte concentration. Furthermore, estimation of the Debye length within the pores filled with organic phase electrolyte show that these lengths are small relative to the radii of the nanopores employed. This discounts wall charge as a contributing factor. Finally, emulsification effects at the ITIES have been alluded to [37,38]; this might occur at the nanoITIES under high flux conditions where a transferring ion undergoes loss/gain of solvation [39] molecules which may contribute to an increased local concentration, e.g. water in the organic phase close to the interface. In such case, the sloped limiting current would vary with pore–pore separation (i.e. r_c/r_a ratio) used to create the nanoITIES array (due to the change in flux), as was reported previously [28,36]. Given the dependence of the sloped limiting current on the aqueous phase electrolyte concentration and not on the organic electrolyte concentration, this points to contributing factors in the aqueous phase.

Furthermore, it is well-known in the literature that Li^+ transfer occurs at the ITIES facilitated by organic-phase anions [40–42], such as the $TBPCl^-$ anion used in this work. This facilitated transfer of Li^+ is evident in the blank voltammograms reported here (Figs. 1A, 3 and 4). The transfer of Li^+ occurs over a broad potential range. As this is electrolyte cation transfer, it results in a loss of supporting electrolyte from the aqueous phase. This means that the experiments for TAA^+ transfer occur in conditions of inadequate supporting electrolyte, the result of which is migration combined with diffusion, or ternary electrodiffusion [27,43–46]. This observation is also in agreement with the issue of whether electroneutrality at the ITIES is a valid assumption [47]. This occurrence of ternary electrodiffusion provides an explanation of why the sloped limiting current slope changes with aqueous phase electrolyte concentration but shows no apparent dependence on the concentration of the organic phase electrolyte; i.e. there is loss of electrolyte from the aqueous phase that leads to under-supported local conditions. Hence, the migrational enhancement introduced by ternary electrodiffusion occurs on the aqueous side of the ITIES and not in the organic phase which is held within the confines of the nanopores used to support the nanoITIES. It will be interesting to test in due course if this hypothesis holds also for aqueous electrolytes with other cations (e.g. sodium or potassium cations).

4. Conclusion

An investigation into the observed sloped limiting current region seen with nanoITIES formed at silicon nitride nanoporous membranes was undertaken. Experimental results show clearly a sloped limiting current for the transfer of various alkylammonium cations and is evident across a range of potentials associated with the transfer of the alkylammonium cations. Systematic variation of the aqueous or organic phase electrolyte concentrations shows that the observed responses are linked to the concentration of aqueous phase electrolyte. Based on voltammograms of nanoITIES arrays with only electrolytes present (i.e. no analyte ion transfer), it is shown that currents consistent with cation transfer from aqueous phase electrolyte to organic phase electrolyte are obtained, in agreement with reports in the literature that Li^+ cations undergo transfer facilitated by the organic phase electrolyte anion, $TPBCl^-$. This loss of cations from the aqueous phase leads to insufficient concentrations of aqueous electrolyte, i.e. unsupported conditions. The sloped limiting currents recorded for alkylammonium cation transfer are accordingly linked to electrodiffusion-controlled transfers.

The implications of the results presented here are that nanoITIES array experiments are always distorted by the presence of both analyte and background electrolyte transfers. As the analyte transfer is also combined with electrolyte transfer, commonly used methods such as background subtraction might not always be a viable approach, especially when the objective is to extract some fundamental information that is not otherwise externally calibrated. Finally, and in agreement with the observations of others, background electrolyte transfer occurs across a range of potentials. This transfer is enhanced at nanopore-based ITIES.

CRediT authorship contribution statement

Mickaël Rimboud: Writing – review & editing, Writing – original draft, Methodology, Investigation, Conceptualization. **Benjamin J.J. Austen:** Writing – original draft, Investigation, Conceptualization. **Jörg Strutwolf:** Writing – review & editing, Investigation. **Yang Liu:** Writing – review & editing, Investigation. **Damien W.M. Arrigan:** Writing –

review & editing, Supervision, Methodology, Funding acquisition, Conceptualization.

Declaration of competing interest

The authors declare the following financial interests/personal relationships which may be considered as potential competing interests: Damien W. M. Arrigan reports financial support was provided by Australian Research Council. If there are other authors, they declare that they have no known competing financial interests or personal relationships that could have appeared to influence the work reported in this paper.

Acknowledgments

This work was supported in various parts by Curtin University and the Australian Research Council (DP130102040). BJJA acknowledges support of the Australian Government Research Training Program Scholarship and the Rowe Scientific Scholarship.

References

[1] S.J. Liu, Q. Li, Y.H. Shao, Electrochemistry at micro- and nanoscopic liquid/liquid interfaces, Chem. Soc. Rev. 40 (2011) 2236–2253.
[2] G. Herzog, Recent developments in electrochemistry at the interface between two immiscible electrolyte solutions for ion sensing, Analyst 140 (2015) 3888–3896.
[3] H.D. Jetmore, E.S. Anupriya, T.J. Cress, M. Shen, Interface between two immiscible electrolyte solutions electrodes for chemical analysis, Anal. Chem. (2022) 16519–16527.
[4] D.W.M. Arrigan, E. Alvarez de Eulate, Y. Liu, Electroanalytical opportunities derived from ion transfer at interfaces between immiscible electrolyte solutions, Aust. J. Chem. 69 (2016) 1016–1032.
[5] D. Homolka, L.Q. Hung, A. Hofmanova, M.W. Khalil, J. Koryta, V. Marecek, Z. Samec, S.K. Sen, P. Vanysek, J. Weber, M. Brezina, M. Janda, I. Stibor, Faradaic ion transfer across the interface of 2 immiscible electrolyte solutions - chronopotentiometry and cyclic voltammetry, Anal. Chem. 52 (1980) 1606–1610.
[6] H.J. Lee, P.D. Beattie, B.J. Seddon, M.D. Osborne, H.H. Girault, Amperometric ion sensors based on laser-patterned composite polymer membranes, J. Electroanal. Chem. 440 (1997) 73–82.
[7] C.B. Milton, K.R. Xu, M. Shen, Recent advances in nanoelectrochemistry at the interface between two immiscible electrolyte solutions, Curr. Opin. Electrochem. 34 (2022).
[8] G. Taylor, H.H.J. Girault, Ion transfer reactions across a liquid-liquid interface supported on a micropipette tip, J. Electroanal. Chem. 208 (1986) 179–183.
[9] Y. Shao, M.D. Osborne, H.H. Girault, Assisted ion transfer at micro-ITIES supported at the tip of micropipettes, J. Electroanal. Chem. 318 (1991) 101–109.
[10] Q. Li, S.B. Xie, Z.W. Liang, X. Meng, S.J. Liu, H.H. Girault, Y.H. Shao, Fast ion-transfer processes at nanoscopic liquid/liquid interfaces, Angew. Chem., Int. Ed. 48 (2009) 8010–8013.
[11] R. Zazpe, C. Hibert, J. O'Brien, Y.H. Lanyon, D.W.M. Arrigan, Ion-transfer voltammetry at silicon membrane-based arrays of micro-liquid-liquid interfaces, Lab Chip 7 (2007) 1732–1737.
[12] M.D. Scanlon, J. Strutwolf, A. Blake, D. Iacopino, A.J. Quinn, D.W.M. Arrigan, Ion-transfer electrochemistry at arrays of nanointerfaces between immiscible electrolyte solutions confined within silicon nitride nanopore membranes, Anal. Chem. 82 (2010) 6115–6123.
[13] M. Sairi, N. Chen-Tan, G. Neusser, C. Kranz, D.W.M. Arrigan, Electrochemical characterisation of nanoscale liquid liquid interfaces located at focused ion beammilled silicon nitride membranes, ChemElectroChem 2 (2015) 98–105.
[14] B. Kralj, R.A.W. Dryfe, Membrane voltammetry: The interface between two immiscible electrolyte solutions, PCCP 3 (2001) 5274–5282.
[15] M.D. Scanlon, D.W.M. Arrigan, Enhanced electroanalytical sensitivity via interface miniaturisation: ion transfer voltammetry at an array of nanometre liquid-liquid interfaces, Electroanalysis 23 (2011) 1023–1028.
[16] M. Rimboud, R.D. Hart, T. Becker, D.W.M. Arrigan, Electrochemical behaviour and voltammetric sensitivity at arrays of nanoscale interfaces between immiscible liquids, Analyst 136 (2011) 4674–4681.
[17] M. Sairi, J. Strutwolf, R.A. Mitchell, D.S. Silvester, D.W.M. Arrigan, Chronoamperometric response at nanoscale liquid-liquid interface arrays, Electrochim. Acta 101 (2013) 177–185.
[18] Y. Liu, J. Strutwolf, D.W.M. Arrigan, Ion-transfer voltammetric behavior of propranolol at nanoscale liquid-liquid interface arrays, Anal. Chem. 87 (2015) 4487–4494.
[19] H. Katano, H. Tatsumi, M. Senda, Ion-transfer voltammetry at 1,6-dichlorohexane|water and 1,4-dichlorobutane|water interfaces, Talanta 63 (2004) 185–193.
[20] M. Rimboud, C. Elleouet, F. Quentel, M. L'Her, Potential scale for ion transfers at the water vertical bar 1,6-dichlorohexane interface, Electrochim. Acta 55 (2010) 2513–2517.
[21] Y. Saito, A theoretical study on the diffusion current at the stationary electrodes of circular and narrow band types, Rev. Polarogr. 15 (1968) 177–187.
[22] A.M. Bond, D. Luscombe, K.B. Oldham, C.G. Zoski, A comparison of the chronoamperometric response at inlaid and recessed disk microelectrodes, J. Electroanal. Chem. 249 (1988) 1–14.
[23] N. Godino, X. Borrise, F.X. Munoz, F.J. del Campo, R.G. Compton, Mass transport to nanoelectrode arrays and limitations of the diffusion domain approach: theory and experiment, J. Phys. Chem. C 113 (2009) 11119–11125.
[24] Z. Koczorowski, G. Geblewicz, Electrochemical studies of the tetrabutylammonium and tetramethylammonium ion transfer across the water-1,2-dichloroethane interface - a comparison with the water-nitrobenzene interface, J. Electroanal. Chem. 139 (1982) 177–191.
[25] T. Wandlowski, V. Marecek, Z. Samec, Galvani potential scales for water-nitrobenzene and water-1,2-dichloroethane interfaces, Electrochim. Acta 35 (1990) 1173–1175.
[26] J. Langmaier, K. Stejskalova, Z. Samec, Evaluation of the standard ion transfer potentials for PVC plasticized membranes from voltammetric measurements, J. Electroanal. Chem. 496 (2001) 143–147.
[27] S. Wilke, T. Zerihun, Diffusion effects at microhole supported liquid/liquid interfaces, Electrochim. Acta 44 (1998) 15–22.
[28] Y. Liu, M. Sairi, G. Neusser, C. Kranz, D.W.M. Arrigan, Achievement of diffusional independence at nanoscale liquid liquid interfaces within arrays, Anal. Chem. 87 (2015) 5486–5490.
[29] S.E.C. Dale, P.R. Unwin, Polarised liquid/liquid micro-interfaces move during charge transfer, Electrochem. Commun. 10 (2008) 723–726.
[30] G.C. Gschwend, A. Olaya, H.H. Girault, How to polarise an interface with ions: the discrete Helmholtz model, Chem. Sci. 11 (2020) 10807–10813.
[31] R.A. Robinson, R.H. Stokes, Electrolyte Solutions, 2nd ed., Butterworths, London, 1959.
[32] J.A. Banait, K.S. Sidhu, J.S. Walia, Transference numbers and solvation studies in n-butanol, Can. J. Chem. 62 (1984) 303–305.
[33] J. Langmaier, A. Trojánek, Z. Samec, Use of the 1,1′-dimethylferrocene oxidation process for the calibration of the reference electrode potential in organic solvents immiscible with water, J. Electroanal. Chem. 616 (2008) 57–63.
[34] A.K. Kontturi, K. Kontturi, J.A. Manzanares, S. Mafé, L. Murtomäki, Ion pairing in the analysis of voltammetric data at the ITIES: RbTPB and RbTPBCl in 1,2-dichloroethane, Berichte der Bunsengesellschaft für physikalische Chemie 99 (1995) 1131–1136.
[35] M. Rimboud, K. Charreteur, V. Sladkov, C. Elleouet, F. Quentel, M. L'Her, Effect of the supporting electrolytes on voltammetry at liquid/liquid microinterfaces between water and nitrobenzene, 1,2-dichloroethane or 1,6-dichlorohexane, J. Electroanal. Chem. 636 (2009) 53–59.
[36] Y. Liu, R. Moshrefi, W.D.A. Rickard, M.D. Scanlon, T.J. Stockmann, D.W. M. Arrigan, Ion-transfer electrochemistry at arrays of nanoscale interfaces between two immiscible electrolyte solutions arranged in hexagonal format, J. Electroanal. Chem. 909 (2022) 116113.
[37] H.H. Girault, Hard science at soft interfaces, in: D. Pletcher, Z.-.-Q. Tian, D. E. Williams (Eds.), Developments in Electrochemistry, Wiley, Chichester, 2014, pp. 295–308.
[38] H.H. Girault, Electrochemistry at liquid-liquid interfaces, in: A.J. Bard, C.G. Zoski (Eds.), Electroanalytical Chemistry, a Series of Advances, CRC Press, Boca Raton, 2010, pp. 1–104.
[39] K.J. Schweighofer, I. Benjamin, Transfer of small ions across the water/1,2-dichloroethane interface, J. Phys. Chem. 99 (1995) 9974–9985.
[40] Y.H. Shao, M.V. Mirkin, Voltammetry at micropipet electrodes, Anal. Chem. 70 (1998) 3155–3161.
[41] P. Sun, F.O. Laforge, M.V. Mirkin, Ion transfer at nanointerfaces between water and neat organic solvents, J. Am. Chem. Soc. 127 (2005) 8596–8597.
[42] M.F. Suarez-Herrera, M.D. Scanlon, On the non-ideal behaviour of polarised liquid-liquid interfaces, Electrochim. Acta 328 (2019) 135110.
[43] B. Quinn, R. Lahtinen, L. Murtomaki, Simultaneous ion transfer across the microhole ITIES: An example of ternary electrodiffusion, J. Electroanal. Chem. 460 (1999) 149–159.
[44] K.B. Oldham, Theory of steady-state voltammetry without supporting electrolyte, J. Electroanal. Chem. 337 (1992) 91–126.
[45] S. Wilke, Current–potential curves for liquid|liquid microinterfaces with no added supporting electrolyte in the water phase, J. Electroanal. Chem. 504 (2001) 184–194.
[46] F. Li, Y. Chen, M. Zhang, P. Jing, Z. Gao, Y. Shao, Ion transfer reactions in media of low ionic strength, J. Electroanal. Chem. 579 (2005) 89–102.
[47] A. Molina, J.M. Olmos, E. Laborda, General theoretical treatment of simple and facilitated ion transfer processes at the most common liquid/liquid microinterfaces, Sens. Actuators B-Chemi. 253 (2017) 326–334.